The Torsional Potential of Dimethyl Peroxide: Still a Difficult Case for Theory

Somsak Tonmunphean,[†] Vudhichai Parasuk,[†] and Alfred Karpfen*[,‡]

Department of Chemistry, Faculty of Science, Chulalongkorn University, Patumwan, Bangkok, 10330 Thailand, and Institute for Theoretical Chemistry und Molecular Structural Biology, University of Vienna, Währinger Strasse 17, A-1090 Vienna, Austria

Received: September 12, 2001; In Final Form: November 6, 2001

The torsional potential about the O−O single bond of dimethyl peroxide, CH_3OOCH_3, was investigated with the aid of large-scale ab initio calculations performed at different levels of Møller−Plesset perturbation theory and coupled-cluster expansions. Additionally, several density functional approaches were applied. For comparative purposes, the torsional potentials of methyl hydroperoxide, CH_3OOH, and hydrogen peroxide, HOOH, were calculated at the same levels of approximation. In the already well-investigated case of HOOH and also for CH_3OOH excellent agreement with the experimentally determined structures and barrier heights can be achieved at the coupled-cluster CCSD(T) level with the application of extended polarized basis sets augmented with diffuse functions. However, in the case of dimethyl peroxide, the peculiar shape of the computed CCSD(T)/cc-pVTZ torsional potential, with an exceedingly shallow region ranging from 110 to 250°, with two skew minima at about 115 and 245° and with a trans minimum at 180°, deviates significantly from that of the experimentally derived torsional potential, which has a barrier at 180° separating the two distinctly deeper skew minima at 120 and 240°. The difficulties encountered in reaching a reasonably converged result with respect to further basis set extension are discussed. It is also shown that the results of density functional theory (DFT) and Møller−Plesset second-order (MP2) calculations differ considerably from the Møller−Plesset higher-order and CCSD(T) results.

1. Introduction

The molecular structures of the simple peroxide molecules ROOR′, with R and R′ being either H or CH_3, have attracted considerable attention over the past decades. This is partly due to difficulties encountered in early attempts to describe the equilibrium structure of the three molecules in this series, hydrogen peroxide (HOOH), methyl hydroperoxide (CH_3OOH), and dimethyl peroxide (CH_3OOCH_3), at one uniform level of approximation.[1,2] The most sensitive structural parameter in these three molecules is the ROOR′ dihedral angle.

The case of HOOH has already been extensively discussed in the literature. A very large number of theoretical calculations has been devoted to the computation of the equilibrium structure, barrier heights, structures at the planar cis and trans conformations, shape of the entire torsional potential, global 6D potential surface, and vibrational and rotational spectroscopic quantities.[1−25] From the experimental side, a trans barrier of 387 cm^{-1} [26−28] (1 kcal mol^{-1} = 349.755 cm^{-1}) and values for the cis barrier of 2460,[26] 2488,[27] and 2563[28] cm^{-1} have been reported.

Considerably fewer calculations have been performed on the structure of the CH_3OOH molecule,[1,2,29−35] and the relative energetics of the stationary points has been dealt with in only a few of them.[1,2,30] However, from an analyis of microwave and millimeter-wave spectra,[30] a skew minimum structure and a barrier height to the trans saddle point of 172.5 cm^{-1} have already been reported.

The most difficult species in this series is CH_3OOCH_3. Early photoelectron spectroscopic data were interpreted in favor of a planar trans or near-planar COOC configuration,[36,37] whereas the analysis of infrared and Raman data[38,39] pointed to a nonplanar COOC backbone structure with C_2 symmetry. To the best of our knowledge, no microwave structure of this molecule has yet been published. The currently widely accepted experimental geometry of dimethyl peroxide stems from an electron diffraction investigation by Haas and Oberhammer.[40] This investigation resulted in a skew equilibrium dihedral COOC angle of 119 ± 10° and an estimate of the trans barrier of about 0.25 kcal mol^{-1} (87 cm^{-1}). The theoretical calculations published so far lead to conflicting results as to the equilibrium torsional angle of dimethyl peroxide,[1,2,41−44] with predicted values close to either a skew configuration of 120° or a trans arrangement of 180°. A more extended compilation of earlier theoretical results was reported by Oberhammer.[45] In that paper, CH_3OOCH_3 is mentioned explicitely as a molecule for which it was difficult to bring experimental and theoretical results into agreement with each other.

In this work, we systematically investigated the torsional potentials of HOOH, CH_3OOH, and CH_3OOCH_3. To gain an understanding of the convergence behavior, the calculations were performed with many different basis sets ranging to very extended basis sets augmented with low-exponent, diffuse, and

TABLE 1: Fitted Potential Parameters for the HOOH Torsional Potential of Hydrogen Peroxide as Obtained with the aug-cc-pVQZ Basis Set[a]

method	V_1	V_2	V_3	V_4
B3LYP	2058.88	−1250.24	84.92	−1.01
MP2	2120.38	−1313.86	90.82	−3.23
CCSD(T)//MP2	2046.54	−1285.98	86.20	−3.24

[a] All values in cm^{-1}.

* Author to whom correspondence should be addressed. Tel.: (+43-1) 4277-52760. Fax: (+43-1) 4277-9527. E-mail: Alfred.Karpfen@univie.ac.at.
† Chulalongkorn University.
‡ University of Vienna.

10.1021/jp013488e CCC: $22.00 © 2002 American Chemical Society
Published on Web 12/13/2001

TABLE 2: Calculated Equilibrium Structures of Methyl Hydroperoxide[a]

Bond Lengths							
basis set	method	R(C−O)	R(O−O)	R(O−H)	R(C−H$_1$)	R(C−H$_2$)	R(C−H$_3$)
cc-pVDZ	B3LYP	1.4143	1.4532	0.9741	1.1019	1.1043	1.1059
	MP2	1.4149	1.4582	0.9720	1.1014	1.1034	1.1048
	CCSD(T)	1.4195	1.4687	0.9726	1.1052	1.1068	1.1085
aug-cc-pVDZ	B3LYP	1.4205	1.4542	0.9701	1.0987	1.0998	1.1009
	MP2	1.4278	1.4724	0.9726	1.1002	1.1009	1.1018
	CCSD(T)	1.4322	1.4785	0.9725	1.1043	1.1045	1.1059
cc-pVTZ	B3LYP	1.4146	1.4530	0.9666	1.0907	1.0919	1.0933
	MP2	1.4129	1.4514	0.9658	1.0878	1.0888	1.0900
aug-cc-pVTZ	B3LYP	1.4163	1.4542	0.9669	1.0903	1.0915	1.0927
	MP2	1.4162	1.4566	0.9678	1.0885	1.0895	1.0903
cc-pVQZ	B3LYP	1.4140	1.4505	0.9655	1.0898	1.0911	1.0924
Bond Angles							
basis set	method	∠COO	∠OOH	∠OCH$_1$	∠OCH$_2$	∠OCH$_3$	
cc-pVDZ	B3LYP	106.2	99.8	104.6	111.6	111.9	
	MP2	105.0	98.5	104.7	111.4	111.7	
	CCSD(T)	105.0	98.8	104.8	111.4	111.7	
aug-cc-pVDZ	B3LYP	106.4	100.6	104.3	110.9	111.4	
	MP2	104.6	99.0	104.3	110.6	111.1	
	CCSD(T)	104.8	99.5	104.4	111.0	111.5	
cc-pVTZ	B3LYP	106.5	100.4	104.7	111.2	111.6	
	MP2	105.1	99.2	104.8	111.0	111.5	
aug-cc-pVTZ	B3LYP	106.6	100.6	104.5	111.1	111.5	
	MP2	105.0	99.3	104.5	110.7	111.2	
cc-pVQZ	B3LYP	106.6	100.6	104.6	111.2	111.6	
Torsional Angles							
basis set	method	∠COOH	∠OOCH$_1$	∠OOCH$_2$	∠OOCH$_3$		
cc-pVDZ	B3LYP	117.7	177.5	59.2	296.2		
	MP2	118.8	177.6	59.1	296.4		
	CCSD(T)	117.2	177.6	59.1	296.4		
aug-cc-pVDZ	B3LYP	118.2	177.2	59.0	295.9		
	MP2	117.6	177.2	58.8	296.1		
	CCSD(T)	112.6	177.3	58.8	296.1		
cc-pVTZ	B3LYP	116.0	177.3	59.0	296.0		
	MP2	116.5	177.2	58.8	296.1		
aug-cc-pVTZ	B3LYP	118.5	177.2	58.9	295.8		
	MP2	120.2	177.1	58.7	296.0		
cc-pVQZ	B3LYP	116.3	177.9	58.9	295.9		

[a] Bond lengths in Å and angles in degrees. [b] Estimated.

also higher-order polarization functions. Similarly, apart from MP2 and DFT approaches, different Møller−Plesset higher-order and coupled-cluster expansion techniques ranging up to the MP4(SDTQ) and CCSD(T) methods were applied. As far as possible and as far as the available computing facilities allowed, the same set of methods was applied to all three molecules. The data presented should allow for an improved quantitative understanding of the structures and torsional potentials of HOOH and CH_3OOH. Also, for CH_3OOCH_3, the present results should be sufficiently reliable and sufficiently close to the basis set limit to establish the shape of the COOC torsional potential of CH_3OOCH_3, at least within the framework of CCSD(T).

2. Method of Calculation

All quantum chemical calculations were performed with the Gaussian 98 suite of programs.[46] As calculational approaches, the MP2 method[47] and a series of higher-order electron correlation methods up to MP4(SDTQ)[48] and CCSD(T)[49−53] were applied. In addition, several DFT variants (B3LYP,[54−57] BLYP, and PW91PW91[58]) were used for dimethyl peroxide to demonstrate their performance in that delicate case.

As basis sets, the correlation-consistent (aug)-cc-pVnZ[59−64] basis sets of Dunning and co-workers and several of the Pople-type basis sets[65−70] were chosen. Particular emphasis was placed on the use of diffuse functions (aug in the case of Dunning basis sets, ++ in the case of Pople-type basis sets) to minimize the effect of intramolecular basis set superposition error (BSSE) contributions to the torsional potential and also to allow for a correct evaluation of the intramolecular dispersion (nonbonded) contribution to the rotational potential when methyl groups are present.

To generate sufficient points for accurate analytical fitting and for dynamical calculations to be performed at a later stage, and because of the exceedingly flat region around the torsional angle values of 180 ± 70°, particularly in the case of dimethyl peroxide, the ROOR′ torsional potentials were scanned in a rather tight and regular mesh with a stepsize of 10° ranging from 0 to 180°. Full optimization of all remaining geometry parameters was carried at the DFT and MP2 levels. Only for the MP2 calculations with the very largest basis sets were optimized geometries obtained with smaller basis sets used. Post-MP2 scans of the torsional potentials with a given basis set were performed at MP2-optimized geometries obtained with the same basis set. The eventual influence of this approximation was checked by performing CCSD(T) geometry optimizations at the stationary points, when affordable, and was found to be entirely negligible, if compared to the still remaining convergence problems toward the infinite basis set limit or in view of the still-missing higher-order correlation contributions.

3. Results and Discussion

3.1. Hydrogen Peroxide. In the context of this work, HOOH mainly served as a test case for basis set convergence and also for a detailed examination of the trends within the series of post-MP2 methods. Many excellent treatments of the torsional potential and of other properties of this molecule are already available in the literature.

The optimized structures at the equilibrium configuration and at the trans and cis saddle points, as well as the barrier heights at the cis and trans saddle points, obtained with the B3LYP, MP2, and CCSD(T) methods are reported in three tables provided as Supporting Information. Here, only a few general trends are discussed. The calculated CCSD(T) structures and energies obtained with the nonaugmented cc-pVDZ, cc-pVTZ, and cc-pVQZ basis sets are identical to the earlier results of Rendell and Lee[10] and Koput.[13] In general, the difference between MP2- and CCSD(T)-optimized structures is small. Of particular significance for the calculations on the CH_3OOH and CH_3OOCH_3 molecules to be discussed in the following sections is the finding that the CCSD(T) barrier heights obtained at the CCSD(T)-optimized *and* at the MP2-optimized structures differ by less than 5 cm^{-1} with all basis sets. Our best value for the trans barrier, obtained at the CCSD(T)/aug-cc-pVQZ//MP2/aug-cc-pVQZ level, is, at 384 cm^{-1}, in very close agreement with the experimental value[26] of 387 cm^{-1}. In the case of the trans barrier, the CCSD(T)/aug-cc-pVQZ//MP2/aug-cc-pVQZ value of 2517 cm^{-1} is bracketed by the experimental values of 2460[26] and 2488[27] cm^{-1} at the lower side and 2563[28] cm^{-1} at the upper side. The B3LYP barrier heights are, in general, acceptably close to the CCSD(T) barrier heights. MP2 overestimates the cis barriers considerably but produces trans barriers in close agreement with the CCSD(T) results. With the larger basis sets, the B3LYP barrier heights are about 30 ± 10 cm^{-1} below the CCSD(T)-calculated barrier heights. The MP3-, MP4(SDQ)-, and CCSD-calculated cis barriers are very similar and about 25−50 cm^{-1} higher than the CCSD(T) cis barrier. The MP3 trans barrier is almost 50 cm^{-1} above the CCSD(T) trans barrier, i.e., the calculated MP3 minimum is too deep. There is also a small but systematic trend concerning the influence of triple excitations on the trans barrier. The MP4(SDQ) and CCSD values are about 30 cm^{-1} higher than the MP4(SDTQ) and CCSD(T) values.

The aug-cc-pVQZ energies as a function of the HOOH torsional angle τ have been subjected to a simple Fourier fit

$$V(\phi) = \sum_{n=1}^{m} \frac{1}{2} V_n(1 - \cos n\phi)$$

where the angle ϕ is defined as $180 - \tau$. In all cases a simple four-term expansion turned out to be sufficient to reproduce the calculated values (10° mesh) with an accuracy better than 1 cm^{-1}. The resulting V_n values are shown in Table 1. Because of the very close agreement with the experimental barrier heights, the four-term CCSD(T)/aug-cc-pVQZ//MP2/aug-cc-pVQZ Fourier series (last row of Table 1) should provide an accurate representation of the torsional potential of HOOH.

3.2. Methyl Hydroperoxide. In Table 2 are displayed the calculated equilibrium structures of methyl hydroperoxide. The variation in the calculated bond distances with the chosen basis set or with the selected calculational method is modest and quite similar to the case of HOOH. CCSD(T)-calculated O−O distances are 0.01−0.03 Å longer than their B3LYP or MP2 counterparts. For the C−O, O−H, and C−H distances, the differences are even smaller. The calculated COOH torsional angles obtained from full geometry optimizations are in the range of 112.6−120.2°.

TABLE 3: Barrier Heights at the Cis and Trans Saddle Points of Methyl Hydroperoxide[a]

basis set	method	cis	trans
cc-pVDZ	B3LYP	2163	78
	MP2	2318	100
	CCSD(T)//MP2[b]	2286	127
	CCSD(T)	2284	125
aug-cc-pVDZ	B3LYP	2074	114
	MP2	2234	140
	CCSD(T)//MP2	2177	185
	CCSD(T)	2176	184
cc-pVTZ	B3LYP	2060	137
	MP2	2114	117
	MP3//MP2	2069	185
	MP4(SDQ)//MP2	2122	162
	MP4(SDTQ)//MP2	2051	154
	CCSD//MP2	2126	166
	CCSD(T)//MP2	2061	160
aug-cc-pVTZ	B3LYP	2009	111
	MP2	2080	100
	MP3//MP2	2033	176
	MP4(SDQ)//MP2	2087	146
	MP4(SDTQ)//MP2	2014	123
	CCSD//MP2	2068	131
	CCSD(T)//MP2	2024	136
cc-pVQZ	B3LYP	2034	138
	MP2//MP2/cc-pVTZ	2083	104
	MP3//MP2/cc-pVTZ	2038	175
	MP4(SDQ)//MP2/cc-pVTZ	2093	150
aug-cc-pVQZ	MP2//MP2/cc-pVTZ	2062	95
	MP3//MP2/cc-pVTZ	2022	172
	MP4(SDQ)//MP2/cc-pVTZ	2074	142
	experiment	−	172.5[c]

[a] Energies in cm^{-1}. [b] CCSD(T) energies at MP2-optimized structures. [c] Reference 30.

The B3LYP, MP2, CCSD(T) and other selected post-MP2-calculated cis and trans barrier heights are collected in Table 3. Comparisons of the trends in the calculated cis and trans barrier heights of CH_3OOH and HOOH with increasing size of the basis sets are shown in Figures 1 and 2. From these two figures, a number of conclusions can be deduced. (i) The basis set trends are fairly independent of the calculational method chosen. (ii) In agreement with the experimental results, the trans barrier is significantly higher in HOOH than in CH_3OOH by more than 250 cm^{-1}. The potential around the skew minimum is thus considerably shallower in CH_3OOH. The MP2 method, all post-MP2 approaches, and the B3LYP method describe this feature correctly. (iii) All methods agree in predicting that the cis barrier of HOOH is also significantly higher than that of CH_3OOH. The difference amounts to about 500 cm^{-1}. (iv) In the case of the trans barrier of CH_3OOH, the post-MP2 values are bracketed by the MP3 results from above and the MP2 results from below. For HOOH, the MP3-calculated trans barriers are always the highest. The CCSD(T) and MP4(SDTQ) results are, however, always close to the MP2 values. (v) In the case of the cis barrier, the calculated CCSD(T) and MP4(SDTQ) barrier heights are the lowest for both molecules, whereas the MP2 results consistently lie too high by about 100 cm^{-1}.

Because of these quite regular trends, we estimate that CCSD(T)/aug-cc-pVQZ trans and cis barriers should lie at 132 ± 10 and 2010 ± 10 cm^{-1}, respectively. Thus, our best theoretical result for the trans barrier is about 40 cm^{-1} lower than the only available experimental value of 172.5 cm^{-1}.[30]

Analytical Fourier fits were also carried out for the calculated torsional potentials of methyl hydroperoxide. In contrast to the case of HOOH, attempts to reproduce the energies of the ab

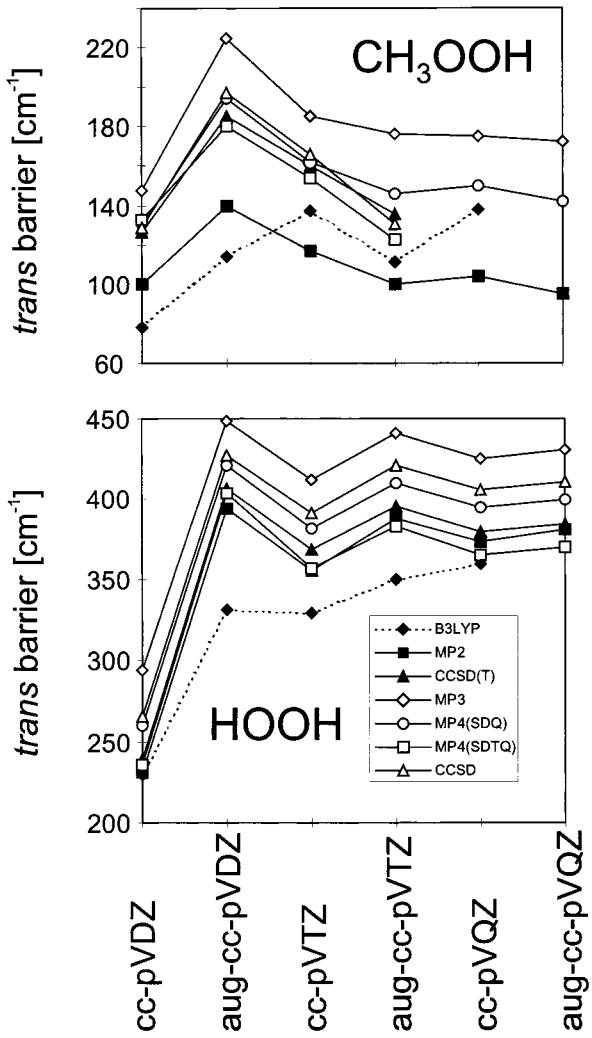

Figure 1. Basis set dependence of trans barrier heights of the torsional potentials of CH_3OOH and HOOH as calculated with the B3LYP, MP2, and post-MP2 methods. MP2/(aug)-cc-pVnZ-optimized geometries were used for the post-MP2 methods. For the (aug)-cc-pVQZ MP2 and post-MP2 calculations, the MP2/cc-pVTZ-optimized geometries were used.

TABLE 4: Fitted Potential Parameters for the COOH Torsional Potential of Methyl Hydroperoxide as Obtained with Different Methods[a]

method[b]	V_1	V_2	V_3	V_4	V_5	V_6
CCSD(T)/cc-pVTZ	1677.33	−1003.9	211.49	−46.68	12.34	−1.49
MP4(SDTQ)cc-pVTZ	1670.23	−995.84	214.16	−48.20	12.76	−1.44
MP4(SDQ)/cc-pVTZ	1731.84	−1035.9	215.44	−42.88	11.28	−1.68
MP4(SDQ)/aug-cc-pVTZ	1741.08	−1000.1	192.16	−34.74	7.18	−1.36
MP4(SDQ)/cc-pVQZ	1733.86	−1010.8	199.72	−32.16	8.91	−1.89

[a] All values in cm^{-1}. [b] At MP2/cc-pVTZ-optimized geometries.

initio points with an accuracy of better than 1 cm^{-1} with the aid of a four-parameter expansion failed. Invariably, deviations of between 10 and 20 cm^{-1} were obtained. However, six-parameter expansions turned out to be sufficient to achieve the desired accuracy. Table 4 contains selected sets of potential parameters obtained from fits to the more advanced calculations. From these fits, we can also narrow the estimated large-basis-set CCSD(T) results for the COOH torsional angle to a value in the region between 113 and 116°. A comparison of our best calculated torsional potentials for HOOH and CH_3OOH is shown in Figure 3.

3.3. Dimethyl Peroxide. In the two previously discussed cases, HOOH and CH_3OOH, methodical improvements led to considerable quantitative, but not qualitative, changes in the calculated torsional potentials. The COOC torsional potential

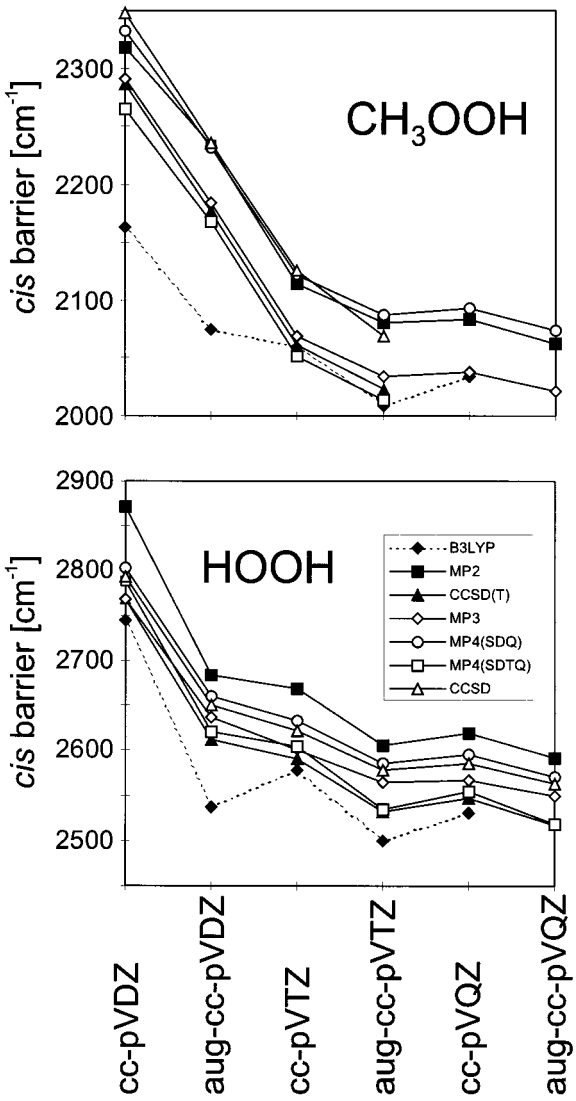

Figure 2. Basis set dependence of cis barrier heights of the torsional potentials of CH_3OOH and HOOH as calculated with the B3LYP, MP2, and post-MP2 methods. MP2/(aug)-cc-pVnZ-optimized geometries were used for the post-MP2 methods. For the (aug)-cc-pVQZ MP2 and post-MP2 calculations, the MP2/cc-pVTZ-optimized geometries were used.

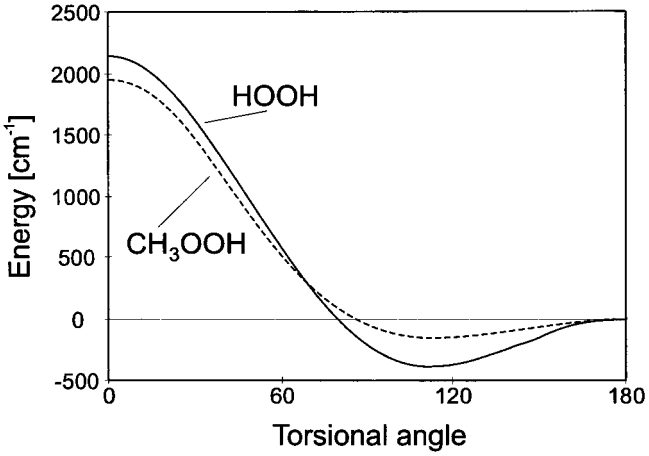

Figure 3. ROOH torsional potentials of hydrogen peroxide and methyl hydroperoxide as obtained from fits to the highest-level calculations performed in this work.

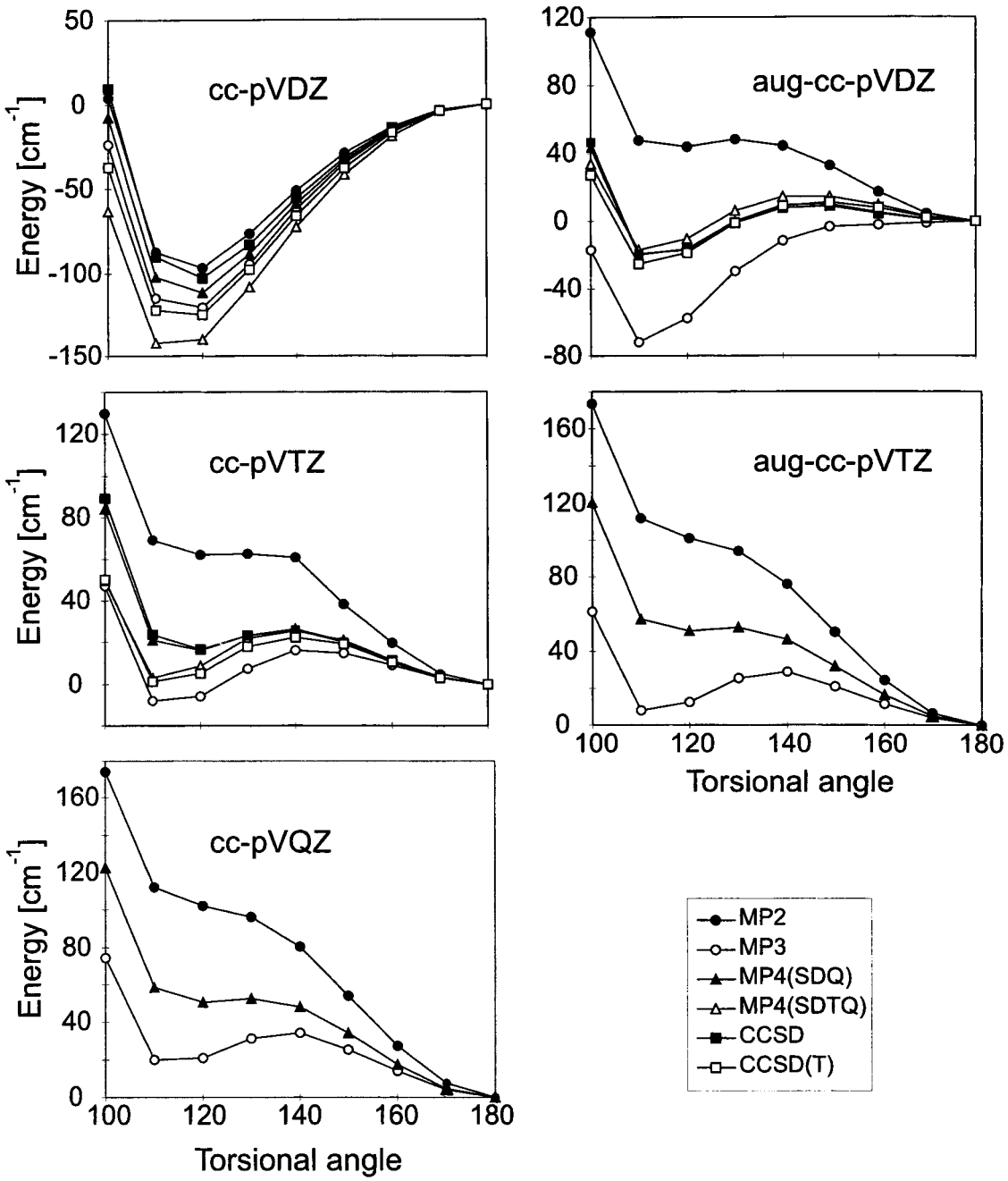

Figure 4. MP2 and post-MP2 COOC torsional potentials of dimethyl peroxide as obtained with Dunning basis sets of increasing size. Only the critical range from 100 to 180° is shown. MP2/(aug)-cc-pVnZ-optimized geometries were used for the post-MP2 methods. For the cc-pVQZ calculations, the MP2/cc-pVTZ-optimized structure was used.

of CH_3OOCH_3, however, constitutes a more subtle problem. The surprising sensitivity to basis set extension and to the electronic structure method applied will be demonstrated in the following. Pointwise-calculated MP2 and post-MP2 torsional potentials of CH_3OOCH_3 obtained at the MP2-optimized structures and with different basis sets are presented in Figures 4 and 5. Only the interesting region between 100 and 180° is shown. Figure 4 contains the results emerging from calculations with the series of Dunning basis sets. Corresponding curves obtained using selected Pople-type basis sets are displayed in Figure 5. Turning first to the series of calculations with Dunning's (aug)-cc-pVnZ basis sets, we observe that the results obtained with the cc-pVDZ basis differ strongly and qualitatively from the larger-basis-set results. With the cc-pVDZ basis, a comparatively deep skew minimum in the vicinity of 110−120° and a saddle point at the trans configuration are obtained for MP2 and all post-MP2 methods. Depending on the method, the calculated trans barrier is between 90 and 150 cm^{-1}. Qualitatively and quantitatively, this shape of the torsional potential would correspond most closely to the one suggested by the electron diffraction experiments[40] with a trans barrier height of 87 cm^{-1}. However, upon systematically increasing the basis set, the shape of the calculated torsional potential changes considerably. The deep skew minimum is flattened, the trans saddle obtained with the cc-pVDZ basis vanishes, and a very flat potential with a minimum at 180° *and* a second, not quite as deep, minimum at the skew conformation develops gradually. The two symmetrically equivalent skew minima are separated by a very low barrier from the trans minimum. Several very systematic method-dependent and basis-set-dependent trends can be observed: (i) From aug-cc-pVDZ to cc-pVQZ, the MP2- and MP3-calculated torsional potentials bracket the higher-order

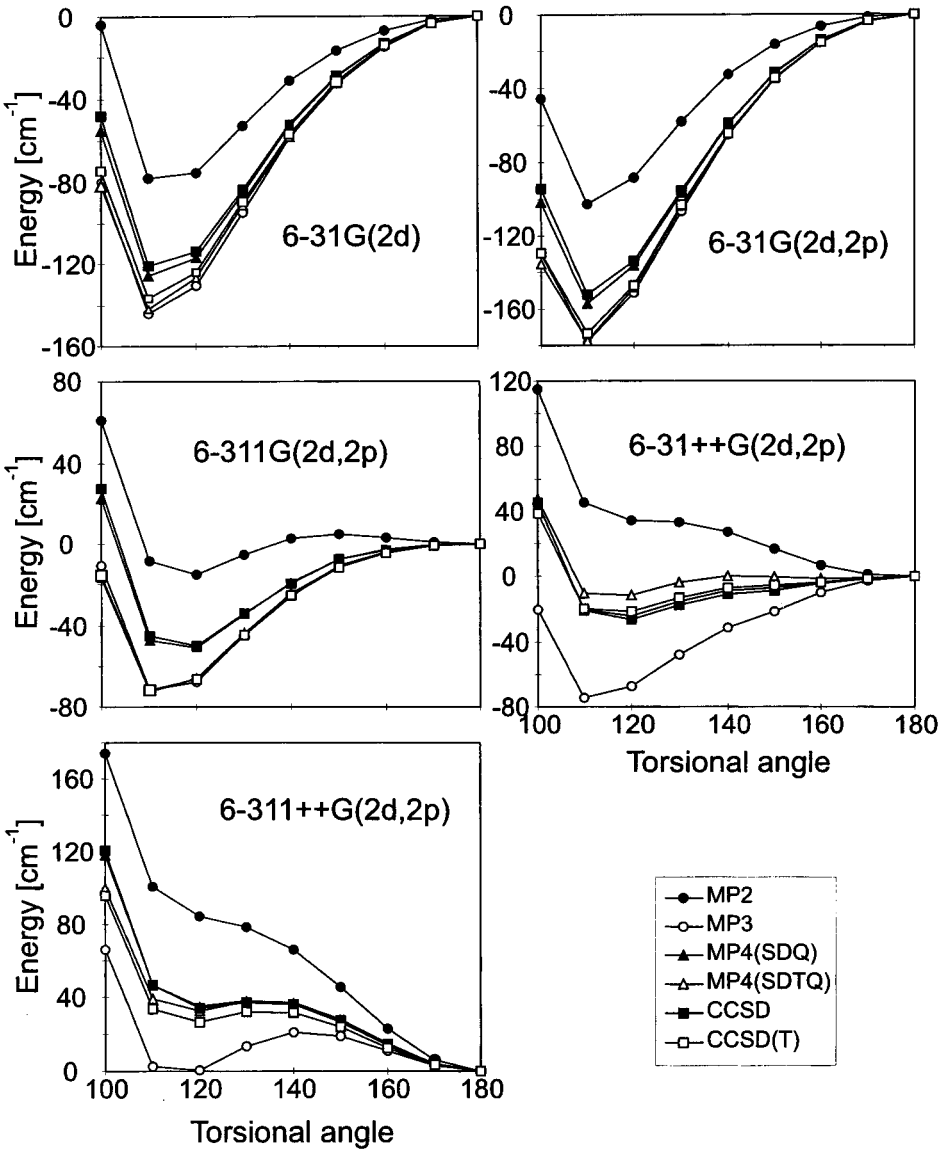

Figure 5. MP2 and post-MP2 COOC torsional potentials of dimethyl peroxide as obtained with Pople-type basis sets of increasing size. Only the critical range from 100 to 180° is shown. For each basis set MP2-optimized geometries were used for the post-MP2 methods.

correlated potential curves, MP2 from above and MP3 from below. For MP2 with the larger basis sets, the skew minimum degenerates to a shoulder only, whereas MP3 displays the triple minimum structure most clearly. (ii) CCSD(T) and MP4(SDTQ) results, where computationally affordable, are close to or slightly below the MP4(SDQ) curves, which, in turn, are practically identical to the CCSD results. (iii) With increasing basis set size, there is a slight tendency to increase the energy of the skew conformation relative to that of the trans structure. (iv) Because of this tendency, the barriers between the trans and the two symmetrically equivalent skew minima tend to become smaller. This leads to extremely shallow skew minima. It is not clear whether these skew minima or the trans minimum can locally sustain a vibrational state. This torsional potential is very far from a harmonic potential. Thus, the initial question of whether dimethyl peroxide has a trans or a skew equilibrium structure has eventually to be answered in the form: *Both* or *neither*! The structure can be described as nonrigid.

The torsional potentials calculated with the Pople basis sets (see Figure 5) show quite similar trends. The 6-31G(2d) and 6-31G(2d,2p) results are qualitatively quite similar to the cc-pVDZ data. The hydrogen p functions have a nonnegligible quantitative effect, lowering the skew minima by about 40 cm^{-1} relative to the energy of the trans structure. Merely changing from 6-31G(2d,2p) to 6-311G(2d,2p) causes a shift in the opposite direction by more than 80 cm^{-1}. Only with the introduction of diffuse functions to the Pople basis sets can one obtain torsional potentials that are qualitatively similar to those resulting from the use of the larger Dunning basis sets. The CCSD(T)/6-311++G(2d,2p) curve is probably within about 20 cm^{-1} of the (for us computationally unattainable) CCSD(T)/aug-cc-pVTZ or CCSD(T)/pVQZ curves. From this finding, one can conclude that, to generate a *converged* torsional potential for dimethyl peroxide, it is most probably more important to use close to saturated spd basis sets, rather than to include higher-order f and g functions. This supposition has, however, not been tested explicitly in this work.

As representative examples, DFT results obtained with the aug-cc-pVTZ basis and with complete geometry optimization are depicted in Figure 6. It is immediately obvious that none of the three functionals used can describe the COOC torsional potential in the critical region. There is no sign of a skew minimum in the DFT//aug-cc-pVTZ-calculated torsional potential curves of dimethyl peroxide.

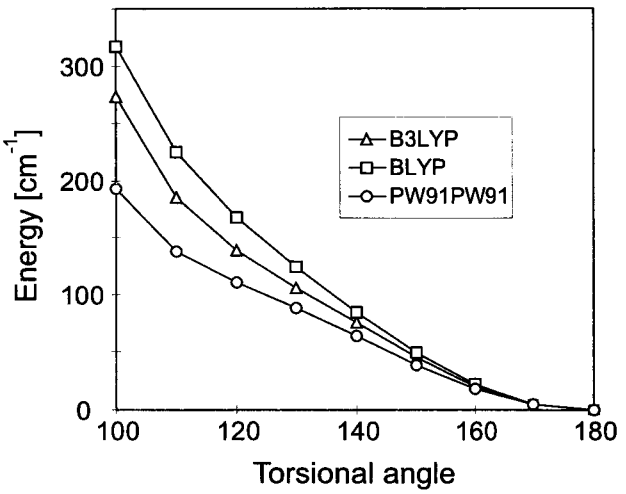

Figure 6. Selected DFT/aug-cc-pVTZ COOC torsional potentials of dimethyl peroxide. Only the critical range from 100 to 180° is shown.

TABLE 5: MP2/cc-pVTZ-Calculated Structures of Dimethyl Peroxide at the Skew, Trans, and Cis Configurations[a]

	skew	trans	cis
	bond lengths		
R(CO)	1.4135	1.4109	1.4096
R(OO)	1.4540	1.4608	1.4771
R(CH$_1$)	1.0879	1.0871	1.0880
R(CH$_2$)	1.0891	1.0896	1.0899
R(CH$_3$)	1.0905	1.0896	1.0899
	bond angles		
∠COO	104.7	103.4	114.9
∠OCH$_1$	104.9	104.9	102.3
∠OCH$_2$	111.1	111.0	113.3
∠OCH$_3$	111.4	111.0	113.3
	torsional angles		
∠COOC	118.8	180.0	0.0
∠OOCH$_1$	178.6	180.0	180.0
∠OOCH$_2$	60.0	61.3	63.5
∠OOCH$_3$	297.3	298.7	296.5

[a] Bond lengths in Å and angles in degrees.

In Table 5, the MP2-optimized structures obtained at the cis, trans, and skew configurations of dimethyl peroxide using the cc-pVTZ basis are compiled. The only sizable structural changes along the torsional path concern the O−O bond distance and the ∠COO bond angle and are mainly caused by relaxations in the more crowded cis structure. Optimized trans and skew geometrical parameters do not differ substantially. The MP2/cc-pVTZ-calculated skew geometrical parameters of dimethyl peroxide and methyl hydroperoxide (see Table 2) are almost indiscernible. Table 6 contains the calculated values for the cis energy barrier. Because of the just discussed uncertainty in the relative energies of trans and skew configurations, the values are reported with the trans energies as a reference only. The cis barrier of dimethyl peroxide is almost twice as large as the cis barrier of methyl hydroperoxide. The methodical trends in the calculated barrier heights are a bit different from those in the two previously discussed molecules, as revealed by a comparison of Figure 7 with Figures 1 and 2. The CCSD(T)- and MP4(SDTQ)-calculated cis barriers are distinctly below the MP2 and the other post-MP2 values, irrespective of the basis set applied. Extrapolation to the infinite basis set limit appears, however, as smooth as for the two smaller peroxides and leads to a cis−trans energy difference slightly above 3800 cm^{-1}. At the current stage, extrapolation of the skew−trans energy difference does not appear meaningful.

TABLE 6: Cis Barrier Heights of Dimethyl Peroxide Relative to the Trans Configuration[a]

basis set	method	cis
cc-pVDZ	B3LYP	3982
	MP2	4238
	CCSD(T)//MP2[b]	4135
aug-cc-pVDZ	B3LYP	3787
	MP2	3944
	CCSD(T)//MP2	3779
cc-pVTZ	B3LYP	3845
	MP2	3988
	MP3//MP2	3934
	MP4(SDQ)//MP2	4013
	MP4(SDTQ)//MP2	3820
	CCSD//MP2	4022
	CCSD(T)//MP2	3825
aug-cc-pVTZ	B3LYP	3826
	MP2// MP2/cc-pVTZ	3954
	MP3//MP2/cc-pVTZ	3908
	MP4(SDQ)//MP2/cc-pVTZ	3990
cc-pVQZ	MP2//MP2/cc-pVTZ	3976
	MP3//MP2/cc-pVTZ	3932
	MP4(SDQ)//MP2/cc-pVTZ	4013
6-311++G(2d,2p)	MP2	4043
	MP3//MP2	3999
	MP4(SDQ)//MP2	4078
	MP4(SDTQ)//MP2	3894
	CCSD//MP2	4083
	CCSD(T)//MP2	3895

[a] Energies in cm^{-1}. [b] CCSD(T) energies at MP2-optimized structures.

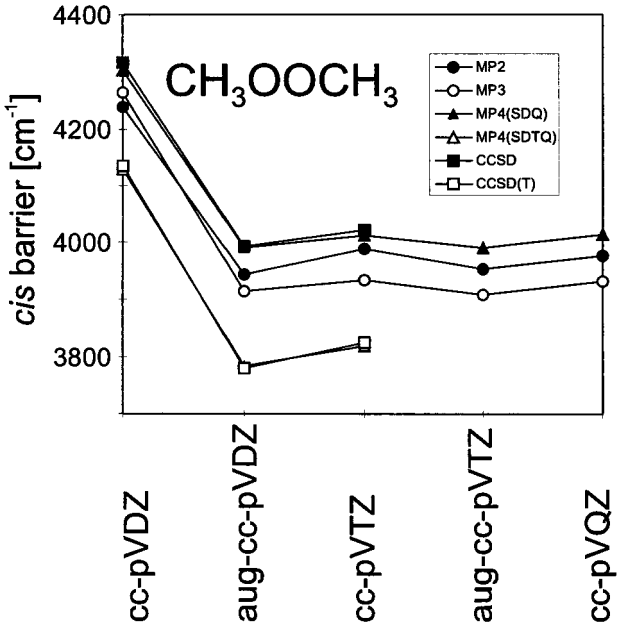

Figure 7. Basis set dependence of cis barrier heights of the torsional potential of CH_3OOCH_3 as calculated with MP2 and post-MP2 methods. MP2/(aug)-cc-pVnZ-optimized geometries were used for the post-MP2 methods. For the cc-pVQZ calculations, the MP2/cc-pVTZ-optimized structure was used.

Attempts to fit the calculated torsional potentials accurately with few-term Fourier series expansions proved to be impossible. Given the flat triple minimum central region of the potential, this is quite understandable. A reasonable result was obtained with a 10-term series. In that case, the points in the region from 100 to 180° could be reproduced with an accuracy of better than 2 cm^{-1}, the remaining points better than 4 cm^{-1}. More extended series did not improve the fits substantially. Moreover, the number of fit parameters would then already approach the number of calculated points. The potential parameters resulting from these fits are shown in Table 7 for a few selected cases.

TABLE 7: Fitted Potential Parameters for the COOC Torsional Potential of Dimethyl Peroxide as Obtained with Different Methods[a]

method[b]	basis set	V_1	V_2	V_3	V_4	V_5	V_6	V_7	V_8	V_9	V_{10}
CCSD(T)	cc-pVTZ	3324.7	−1649.2	422.0	−49.5	79.1	−29.1	−19.7	3.3	17.1	−9.6
MP4(SDQ)	cc-pVTZ	3507.0	−1702.2	432.6	−55.7	76.6	−22.8	−21.1	2.0	16.7	−8.1
MP4(SDQ)	aug-cc-pVTZ	3480.3	−1661.0	443.2	−54.6	73.7	−21.7	−22.8	1.9	15.6	−6.5
MP4(SDQ)	cc-pVQZ	3505.8	−1664.9	435.9	−49.3	75.1	−23.3	−20.7	2.1	15.4	−7.9
CCSD(T)	6-311++G(2d,2p)	3404.5	−1626.6	409.5	−54.7	84.3	−29.5	−20.4	4.7	15.6	−9.4

[a] All values in cm^{-1}. [b] At MP2/cc-pVTZ-optimized geometries.

4. Summary and Conclusions

Large-scale ab initio calculations have been performed with the aim of investigating the torsional potentials of the three simple peroxides HOOH, CH_3OOH, and CH_3OOCH_3 at a reliable level. Because of the very shallow potentials in the region around 180 ± 70°, extended basis sets and higher-order correlation approaches had to be used to reach this goal. The data obtained for HOOH are in excellent agreement with previous literature data from the theoretical side and with the experimentally reported trans and cis barrier heights.

Our results for the torsional potential of CH_3OOH constitute a definite improvement over previous ab initio calculations. In that case, the best calculated trans barrier is with 130 ± 10 cm^{-1}, which is about 40 cm^{-1} below the only available experimental value of 172.5 cm^{-1}, i.e., the calculated skew minimum is less deep than the experiment suggests.

The calculations presented on the torsional potential of dimethyl peroxide far surpass earlier attempts from the theoretical side. Nevertheless, the situation is still unsatisfactory. The most recent and generally accepted experiment, a gas-phase electron diffraction study,[40] was interpreted in terms of a skew minimum and a barrier to the trans saddle point of 0.25 kcal mol^{-1} or 87 cm^{-1}. The detailed scans of the COOC torsional potential performed in this work revealed that this section of the energy surface is exceedingly flat in the region extending from 180 − 70° to 180 + 70°, eventually displaying a triple minimum structure with two very low barriers. From preliminary attempts to extrapolate toward the infinite basis set CCSD(T) limit, it appears that the two skew minima and the trans minimum will still be present. Thus, the feature that the CCSD-(T)-calculated potential is exceedingly shallow in the region around 180 ± 70° will definitely persist.

The picture emerging from our calculations is a COOC torsional coordinate that can be best described as a very large amplitude coordinate, with the consequence that the equilibrium structure of CH_3OOCH_3 is not well defined. This result is not in agreement with the currently accepted experimental structure as derived from gas-phase electron diffraction experiments. In the trans configuration, CH_3OOCH_3 does not have a dipole moment, whereas in the skew configuration, it does. Whether the peculiar structure of the calculated torsional potential in the vicinity of the skew conformation suffices to give rise to an observable rotational spectrum is a question that goes beyond the scope of this work. Similarly, the eventual role of coupling between the rotation about the O−O bond and the two methyl rotations still needs to be explored in future investigations.

Acknowledgment. The calculations were performed on the Cluster of Digital Alpha Servers (2100 4/275) of the computer center of the University of Vienna and on local RISC 6000/550 workstations at the Institute of Theoretical Chemistry and Structural Molecular Biology of the University of Vienna. The authors are grateful for the ample supply of computer time on these installations.

Supporting Information Available: Three tables reporting the optimized structures at the equilibrium configuration of hydrogen peroxide and at the trans and cis saddle points, as well as the barrier heights at the cis and trans saddle points, obtained with the B3LYP, MP2, and CCSD(T) methods. This material is available free of charge via the Internet at http://pubs.acs.org.

References and Notes

(1) Bair, R. A.; Goddard, W. A., III. *J. Am. Chem. Soc.* **1982**, *104*, 2719.
(2) Christen, D.; Mack, H.-G.; Oberhammer, H. *Tetrahedron* **1988**, *44*, 7363.
(3) Cremer, D. *J. Chem. Phys.* **1978**, *69*, 4440.
(4) Cremer, D.; Christen D. *J. Mol. Spectrosp.* **1979**, *74*, 480.
(5) Carpenter, J. E.; Weinhold, F. *J. Phys. Chem.* **1988**, *92*, 4295.
(6) Carpenter, J. E.; Weinhold, F. *J. Phys. Chem.* **1988**, *92*, 4306.
(7) Willets, A.; Gaw, J. F.; Handy, N. C.; Carter S. *J. Mol. Spectrosc.* **1989**, *135*, 370.
(8) Harding, L. B. *J. Phys. Chem.* **1989**, *93*, 8004.
(9) Harding, L. B. *J. Phys. Chem.* **1991**, *95*, 8653.
(10) Rendell, A. P.; Lee, T. J. *J. Chem. Phys.* **1994**, *101*, 400.
(11) Samdal, S.; Mastryukov, V. S.; Boggs, J. E. *J. Mol. Struct.* **1995**, *346*, 350.
(12) Antikainen, J.; Friesner, R.; Leforestier, C. *J. Chem. Phys.* **1995**, *102*, 1270.
(13) Koput, J. *Chem. Phys. Lett.* **1995**, *236*, 516.
(14) Chung-Phillips, A.; Jebber, K. A. *J. Chem. Phys.* **1995**, *102*, 7080.
(15) Koput, J. *Chem. Phys. Lett.* **1996**, *57*, 36.
(16) Jursic, B. S. *J. Mol. Struct. (THEOCHEM)* **1997**, *401*, 45.
(17) Jursic, B. S. *J. Mol. Struct. (THEOCHEM)* **1997**, *417*, 81.
(18) Koput, J.; Carter, S.; Handy, N. C. *J. Phys. Chem. A* **1998**, *102*, 6325.
(19) Dobado, J. A.; Molina, J. M.; Olea, D. P. *J. Mol. Struct. (THEOCHEM)* **1998**, *433*, 181.
(20) Gutièrrez-Oliva, S.; Letelier, J. R.; Toro-Labbé, A. *Mol. Phys.* **1999**, *96*, 61.
(21) Kuhn, B.; Rizzo, T. R.; Luckhaus, D.; Quack, M.; Suhm, M. A. *J. Chem. Phys.* **1999**, *111*, 2565.
(22) Chen, R.; Ma, G.; Guo, H. *Chem. Phys. Lett.* **2000**, *320*, 567.
(23) Carter, S.; Handy, N. C. *J. Chem. Phys.* **2000**, *113*, 987.
(24) Benderskii, V. A.; Irgibaeva, I. S.; Vetoshkin, E. V.; Trommsdorff, H. P. *Chem. Phys.* **2000**, *262*, 369.
(25) Senent, M. L.; Fernández-Herrera, S.; Smeyers, Y. G. *Spectrochim. Acta A* **2000**, *56*, 1457.
(26) Hunt, R. H.; Leacock, R. A.; Peters, C. W.; Hecht, K. T. *J. Chem. Phys.* **1965**, *42*, 1931.
(27) Koput, J. *J. Mol. Spectrosc.* **1986**, *115*, 438.
(28) Flaud, J.-M.; Camy-Peyret, C.; Johns, J. W. C.; Carli, B. *J. Chem. Phys.* **1989**, *91*, 1504.
(29) Koller, J.; Hodoscek, M.; Plesnicar, B. *J. Am. Chem. Soc.* **1990**, *112*, 2124.
(30) Tyblewski, M.; Ha, T.-K.; Meyer R.; Bauder, A. *J. Chem. Phys.* **1992**, *97*, 6168.
(31) Bach, R. D.; Owensby, A. L.; Gonzalez, C.; Schlegel, H. B.; McDouall, J. J. W. *J. Am. Chem. Soc.* **1991**, *113*, 6001.
(32) Schalley, C. A.; Dieterle, M.; Schröder, D.; Schwarz, H.; Uggerud, E. *Int. J. Mass Spectrom. Ion Processes* **1997**, *163*, 101.
(33) Schalley, C. A.; Harvey, J. N.; Schröder, D.; Schwarz, H. *J. Phys. Chem. A* **1998**, *102*, 1021.
(34) Aschi, M.; Attinà, M.; Cacace, F.; Cipollini, R.; Pepi, F. *Inorg. Chim. Acta* **1998**, *275−276*, 192.
(35) Messer, B. M.; Stielstra, D. E.; Cappa, C. D.; Scholtens, K. W.; Elrod, M. J. *Int. J. Mass Spectrom.* **2000**, *197*, 219.
(36) Kimura, K.; Osafune, K. *Bull. Chem. Soc. Jpn.* **1975**, *48*, 2421.
(37) Rademacher P.; Elling, W. *Liebigs Ann. Chem.* **1979**, 1473.

(38) Christe, K. O. *Spectrochim. Acta A* **1971**, *27*, 463.
(39) Butwill Bell, M. E.; Laane, J. *Spectrochim. Acta A* **1972**, *28*, 2239.
(40) Haas, B.; Oberhammer, H. *J. Am. Chem. Soc.* **1984**, *106*, 6146.
(41) Gase, W.; Boggs, J. E. *J. Mol. Struct.* **1984**, *116*, 207.
(42) Fournier, R.; DePristo, A. E. *J. Chem. Phys.* **1991**, *96*, 1183.
(43) Huang, M.-B.; Suter, H. U. *J. Mol. Struct. (THEOCHEM)* **1994**, *337*, 173.
(44) Bach, R. D.; Ayala, P. Y.; Schlegel, H. B. *J. Am. Chem. Soc.* **1996**, *118*, 12758.
(45) Oberhammer, H. *J. Comput. Chem.* **1998**, *19*, 123.
(46) Frisch, M. J.; Trucks, G. W.; Schlegel, H. B.; Scuseria, G. E.; Robb, M. A.; Cheeseman, J. R.; Zakrzewski, V. G.; Montgomery, J. A., Jr.; Stratmann, R. E.; Burant, J. C.; Dapprich, S.; Millam, J. M.; Daniels, A. D.; Kudin, K. N.; Strain, M. C.; Farkas, O.; Tomasi, J.; Barone, V.; Cossi, M.; Cammi, R.; Mennucci, B.; Pomelli, C.; Adamo, C.; Clifford, S.; Ochterski, J.; Petersson, G. A.; Ayala, P. Y.; Cui, Q.; Morokuma, K.; Malick, D. K.; Rabuck, A. D.; Raghavachari, K.; Foresman, J. B.; Cioslowski, J.; Ortiz, J. V.; Stefanov, B. B.; Liu, G.; Liashenko, A.; Piskorz, P.; Komaromi, I.; Gomperts, R.; Martin, R. L.; Fox, D. J.; Keith, T.; Al-Laham, M. A.; Peng, C. Y.; Nanayakkara, A.; Gonzalez, C.; Challacombe, M.; Gill, P. M. W.; Johnson, B. G.; Chen, W.; Wong, M. W.; Andres, J. L.; Head-Gordon, M.; Replogle, E. S.; Pople, J. A. *Gaussian 98*, revision A.6; Gaussian, Inc.: Pittsburgh, PA, 1998.
(47) Møller, C.; Plesset, M. S. *Phys Rev.* **1934**, *46*, 618.
(48) Krishnan, R.; Pople, J. A. *Int. J. Quantum Chem.* **1978**, *14*, 91.
(49) Cizek, J. *Adv. Chem. Phys.* **1969**, *14*, 35.
(50) Purvis, G. D.; Bartlett, R. J. *J. Chem. Phys.* **1982**, *76*, 1910.
(51) Scuseria, G. E.; Janssen, C. L.; Schaefer, H. F., III. *J. Chem. Phys.* **1988**, *89*, 7382.
(52) Scuseria, G. E.; Schaefer, H. F., III. *J. Chem. Phys.* **1989**, *90*, 3700.
(53) Pople, J. A.; Head-Gordon, M.; Raghavachari, K. *J. Chem. Phys.* **1987**, *87*, 5968.
(54) Becke, A. D. *Phys. Rev. A* **1988**, *38*, 3098.
(55) Becke, A. D. *J. Chem. Phys.* **1993**, *98*, 5648.
(56) Lee, C.; Yang, W.; Parr, R. G. *Phys. Rev. B* **1988**, *37*, 785.
(57) Mielich, B.; Savin, A.; Stoll, H.; Preuss, H. *Chem. Phys. Lett.* **1989**, *167*, 200.
(58) Perdew, J. P.; Wang, Y. In *Electronic Structure of Solids '91*; Ziesche, P., Eschrig, H., Eds.; Akademie-Verlag: Berlin, 1991.
(59) Dunning, Th. R., Jr. *J. Chem. Phys.* **1989**, *99*, 1007.
(60) Kendall, R. E.; Dunning, Th. R., Jr.; Harrison, R. J. *J. Chem. Phys.* **1992**, *96*, 6796.
(61) Woon, D. E.; Dunning, Th. R., Jr. *J. Chem. Phys.* **1993**, *98*, 1358.
(62) Woon, D. E.; Dunning, Th. R., Jr. *J. Chem. Phys.* **1994**, *100*, 2975.
(63) Woon, D. E.; Dunning, Th. R., Jr. *J. Chem. Phys.* **1995**, *103*, 4572.
(64) Wilson, A. K.; van Mourik, T.; Dunning, Th. R., Jr. **1996**, *388*, 339.
(65) Ditchfield, R.; Hehre, W. J.; Pople, J. A. *J. Chem. Phys.* **1971**, *54*, 724.
(66) Hehre, W. J.; Ditchfield, R.; Pople, J. A. *J. Chem. Phys.* **1972**, *56*, 2257.
(67) McLean, A. D.; Chandler, G. S. *J. Chem. Phys.* **1980**, *72*, 5639.
(68) Frisch, M. J.; Pople, J. A.; Binkley, J. S. *J. Chem. Phys.* **1984**, *80*, 3265.
(69) Krishnan, R.; Binkley, J. S.; Seeger, R.; Pople, J. A. *J. Chem. Phys.* **1980**, *72*, 5639.
(70) Clark, T.; Chandrasekhar, J.; Spitznagel, G. W.; Schleyer, P. v. R. *J. Comput. Chem.* **1983**, *4*, 294.